

Optimal Binding Site of a Methane Molecule on the Silanol Covered (010) Surface of Silicalite-1: ONIOM Calculations

T. Remsungnen,^{*,†} V. Kormilets,[‡] A. Loisuangsin,[§] A. Schüring,[‡] S. Fritzsche,[‡]
R. Haberlandt,[‡] and S. Hannongbua^{*,§}

Department of Mathematics, Faculty of Science, Khon Kaen University, Khon Kaen 40002, Thailand, Department of Molecular Dynamics/Computer Simulation, Faculty of Physics and Geosciences, Institute for Theoretical Physics (ITP), University of Leipzig, Augustusplatz 10-11, 04109 Leipzig, Germany, and Department of Chemistry, Faculty of Science, Chulalongkorn University, Bangkok 10330, Thailand

Received: April 5, 2006

The binding energies and the corresponding structures of a methane molecule on the silanol covered (010) surface of silicalite-1 have been investigated using ab initio methods. Different levels of calculations, HF/6-31G(d), MP2/6-31G(d) and ONIOM (MP2/6-31G(d):HF/6-31G(d)) including the correction of an error due to an unbalance of the basis set, known as basis set super position error (BSSE), as well as the size of the cluster representing the silicalite-1 surface, were systematically examined to validate the model used. The ONIOM method with the BSSE correction was found to be a compromise between accuracy and computer time required. The optimal binding site on the silicalite-1 surface was observed at the configuration where the methane molecule points one H atom toward the O atom of the silanol group. The corresponding binding energy is -1.71 kJ/mol. This value is significantly higher than that of -5.65 kJ/mol when the methane molecule approaches the center of the straight channel. At this configuration, the C atom of methane was observed to locate exactly at the center of the channel. This leads to the conclusion that the methane molecule will relatively seldom be adsorbed on the silanol covered (010) surface of silicalite-1. Instead, the adsorption process will take place directly at the center of the straight channel.

1. Introduction

During the past decades the economical as well as the scientific interest in zeolites increased rapidly. These aluminosilicates contain a regular system of nanosize pores and/or channels and in many cases they also contain exchangeable cations. Therefore, zeolites are used in industries as molecular sieves, catalysts and adsorbents. However, in any one of these applications guest molecules have to enter the zeolite crystallites before diffusing within the pore system. They have to move through the pore opening; i.e., they have to interact with the external surface of the zeolite.

Only recently^{1–15} has the behavior of guest molecules on the zeolite surface been studied. It is known that the surface of most of the zeolitic and amorphous silica materials is covered by silanol groups. Therefore, the interaction with the silanol covered surface is crucial for all applications using the adsorption and diffusion of guest molecules in zeolites.

Most of the information on the characteristics of silanol on the external surface of zeolites arises from FTIR experiments.^{16–24} It was observed that the O–H bond of silanol groups is softened when interacting with nitriles,^{17–20} alcohols,²¹ water,^{22,23,25} pyridine and even with aliphatic and aromatic hydrocarbons.¹⁹

In IR measurements, it has been found that methane molecules are adsorbed at the surface OH groups of a silica surface in remarkable amount only at low temperatures.²⁶ This leads to

the assumption that these OH groups form adsorption centers of low adsorption energy on a silica surface. A weak interaction of methane with OH surface groups has also been found in numerical simulations of methane on silicalite.²⁷ These simulations have been carried out using empirical classical potentials. To our knowledge such measurements for the silicalite surfaces or examinations of this system using ab initio calculations are not available. Therefore, this is one of the aims of the present paper.

Noncationic zeolites, in particular silicalite-1, are widely used in the separation of mixtures between light hydrocarbons and water or other polar solvents because of the hydrophobic nature of the internal surface, whereas its external surface is hydrophilic. The latter property can be attributed to terminal silanol groups that are able to interact with guest molecules. However, most of the experimental and theoretical works focus on the internal surface, the pore or channel, whereas much less is known about the details of the external surface. Recently, the interaction between water molecules and the silanol covered surface of the silicalite-1 was, theoretically, studied.²⁸ Optimal binding sites, binding energies and orientations of water molecules were investigated and discussed in comparison with the experimental data.

In this investigation, the structure and the interaction between methane molecules and the silanol groups on the external surface of silicalite-1 was examined. The energetic and geometric optimizations have been performed using quantum chemical calculations at the HF and MP2 level. A combination of both methods, known as ONIOM (MP2:HF), was also examined to seek an appropriate technique for the investigated system.

* Corresponding authors. E-mail: Supot.h@chula.ac.th (S.H.); rtawun@kku.ac.th (T.R.).

[†] Khon Kaen University.

[‡] University of Leipzig.

[§] Chulalongkorn University.

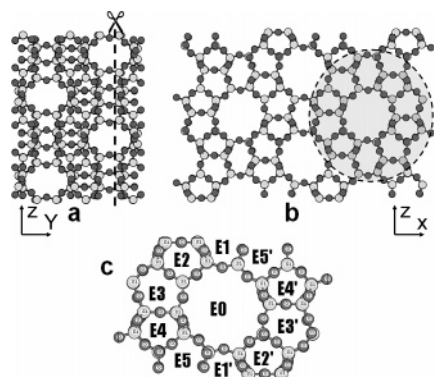


Figure 1. Side-view of the silicalite-1 lattice (a) where the (010) surface was cut along the dashed line and circles. The obtained top-view of the (010) surface can be seen in (b) and (c). The straight channel in (c) was labeled as E0 and the adjacent channels are named as E_i and $E_{i'}$ where $i = i' = 1-5$.

2. Details of the Calculations

2.1. Surface Model of Silicalite-1. The idealized lattice of the MFI framework was obtained from the IZA database.²⁹ The lattice was cut along the dashed line in Figure 1a. The obtained (010) surface (Figure 1b), which is perpendicular to the straight channels, was, again, cut by the circle. The resulting fragment shown in Figure 1c was used for this study. Hydrogen atoms were added to the broken $-\text{Si}-\text{O}-$ bonds. The $\text{Si}-\text{OH}$ and $\text{Si}-\text{H}$ bonds were optimized using quantum chemical calculation at the HF/6-31G(d) level. The obtained $\text{Si}-\text{OH}$ groups were assumed to represent the silanols on the (010) surface of the silicalite-1. For simplicity, an area perpendicular to the straight channel, the 10 oxygen membered ring, was named as an E0 ring and the adjacent channels were labeled as E_i and $E_{i'}$ where $i = i' = 1-5$ (see Figure 1c).

2.2. Test of the ONIOM Method. The high accuracy level, correlated method (MP2) that had been proven to be a feasible method for the calculation of van der Waals complexes^{30,31} and was successfully used in our previous works^{28,32,33} was again applied in this study. On one hand, the system fragment in Figure 1c is still too large to take into account all atoms in the MP2 calculations. On the other hand, use of each single E0–E5 ring will be too small to represent the silicalite-1 (010) surface. Seeking for an optimal compromise between fragment size vs the required computer time, MP2/6-31G(d) and ONIOM-(MP2/6-31G(d):HF/6-31G(d)) calculations were examined. For the quantum MP2/6-31G(d) calculations, the surface was represented by the fragment given in Figure 2a (which is half of the fragment shown in Figure 1c). Then, the methane molecule was located above the centers of the E3 rings and oriented in the configurations where one H atom points away from the center of the ring. The distance between the C atom of methane and the center of the ring was optimized. The binding energy including the basis set superposition error (BSSE) correction was calculated and analyzed.

For the ONIOM calculations, the model part (Figure 2b), which is a subset of the real part and covers the reaction area, the more accurate MP2/6-31G(d) method was applied. However, the real part that covers the whole fragment shown in Figure 2a (including the real part in Figure 2b) was treated by a low level method, HF/6-31G(d). The ONIOM interaction energy of the system, E_{ONIOM} , is derived as

$$E_{\text{ONIOM}} = E_{\text{real,low}} + E_{\text{model,high}} - E_{\text{model,low}} \quad (1)$$

where $E_{\text{real,low}}$ is the total energy of the real system using the

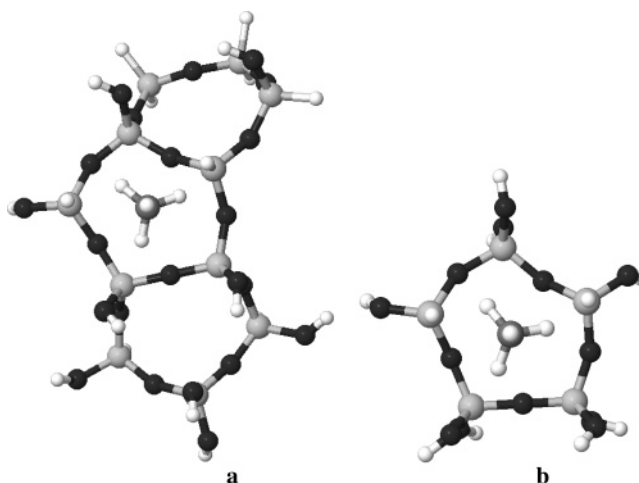


Figure 2. Real (a) and the model (b) parts used for examining the ONIOM method.

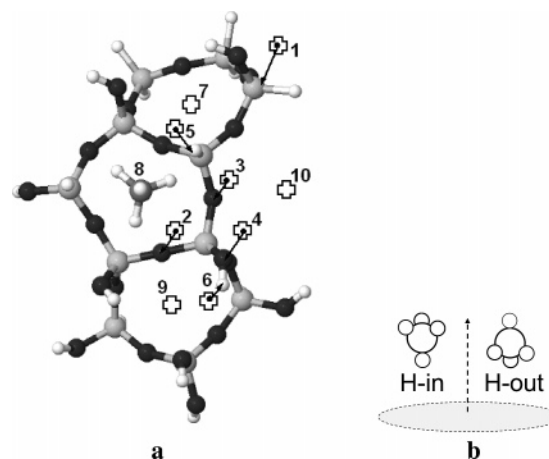


Figure 3. Methane molecule initially located at 2.5 Å above and perpendicular to the points labeled by 1–10 (a) in the two configurations, H-in and H-out (b).

low level method and $E_{\text{model,high}}$ and $E_{\text{model,low}}$ define the total energies of the model part calculated with high and low level methods, respectively.

2.3. Optimal Methane-Surface Binding Energy. To reduce the scope of the calculation, the E1–E5 rings are, respectively, assumed to be identical to the E1'–E5' ones. With this approximation, the methane molecule was assigned to approach the surface only in the first half of the surface shown in Figure 2a. Therefore, the calculations were focused only on the complex structure in the E1–E5 and center of the E0 rings. The methane molecule in the two orientations (H-in and H-out in Figure 3b) was positioned at several points (labeled as 1–10 in Figure 3a), 2.25 Å above the silanol covered surface. The distance from the C atom of the methane molecule to point i , where $i = 1-10$ labeled in Figure 3a, was optimized in the path perpendicular to the surface. The center of mass of all Si atoms of each ring is defined to be the origin of the coordinate frame for the potential calculations on paths 7–10.

The binding energy, ΔE_{bind} , is defined according to the supermolecular approach, as shown in

$$\Delta E_{\text{bind}} = E_{\text{cpx}} - E_{\text{met}} - E_{\text{sur}} \quad (2)$$

where E_{cpx} is the total energy of the complex calculated by the ONIOM method and E_{met} and E_{sur} are the total energies of the methane molecule and of the fragment surface, respectively. All calculations were performed using the GAUSSIAN03 program.³⁴

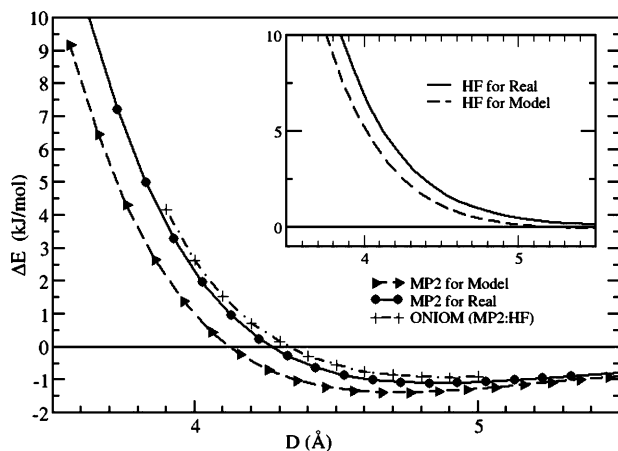


Figure 4. Binding energy including BSSE corrections for the real and model systems (see Figure 2) calculated using MP2 and ONIOM method when the methane molecule is in the configuration H-in (see Figure 3b) and moves perpendicular to the center of the E3 ring (see Figure 3a), where D denotes the distance from the C atom of methane to the center of the E3 ring. The HF calculation is also depicted for comparison.

3. Results and Discussions

3.1. Validity of the Method. According to the calculation details mentioned above where the HF, MP2 and ONIOM interaction energies were evaluated using the partition shown in Figure 2 and the methane molecule was located and moved perpendicular to the E3 rings in the configuration H-in, the results were plotted and compared in Figure 4. Note that the BSSE corrections were taken into account for all data points. From the plots, the following conclusions can be made: (i) The interaction energies (dashed lines in an inset of Figures 4) yielded from the small fragment size (model part, Figure 2b) differ significantly from those of the surface of bigger size (real part, Figure 2a). A clear conclusion is that the small cluster size, such as E3 in Figure 2b, is not enough to represent the calculated system. (ii) Interestingly, the ONIOM (MP2/6-31G(d):HF/6-31G(d)) interaction energies (dotted line in Figure 4) are almost identical to those yielded from the MP2 method (solid line in Figure 4). Note that the bigger fragment in Figure 2a was used in the MP2 calculation.

Taking into account all the data and conclusions given above, the ONIOM (MP2/6-31G(d):HF/6-31G(d)) calculation with the BSSE correction was selected and used throughout to investigate the interaction between the methane molecule and the silanol covered (010) silicalite-1 surface. This is in good agreement with that reported by Sauer et al.³⁵ on the adsorption of the NH_3 and H_2O molecules in acidic chabazite.

3.2. Optimal Binding Site of Methane. In Table 1, the ONIOM binding energies representing the methane/surface interaction in which the surface is represented by the fragment as shown in Figures 3a (equivalent to that in Figure 2a or half of that in Figure 1c) and methane is in the configurations H-in and H-out (see Figure 3b) were summarized. The 10 trajectories are classified into 3 groups where the H-in or H-out configuration of the methane molecule is perpendicular to the atoms (Si, O or H, trajectories 1–6), the center of the small rings (E2–E4, trajectories 7–9) and the center of the 10-membered ring (path 10) of the silicalite-1 surface.

Among the trajectories where the methane molecule points one H atom toward/away from the atoms of the surface, the O atom of the silanol group (path 4 in Table 1 and Figure 3a) was found to be the most favorable binding site. The corresponding binding energy in the H-in configuration is -1.71 kJ/

TABLE 1: Optimal ONIOM Distances (D_{opt} in Å from the C Atom of the Methane Molecule to Point i , Where $i = 1-10$ Labeled in Figure 3a) and the Corresponding Binding Energies (ΔE_{bind} in kJ/mol) Representing the Methane/Surface Interaction in Which the Methane Molecule Points One of the H Atoms toward (H-in) and Away from (H-out) the Surface (Figure 3b)

path i , $i = 1-10$ in Figure 3a	relative orientation H-in		relative orientation H-out	
	D_{opt}	ΔE_{bind}	D_{opt}	ΔE_{bind}
H of CH_4 Points toward/Away from the Atom				
1. Si	5.00	-1.36	5.00	-1.15
2. O of Si-O-Si	4.90	-1.51	4.70	-1.62
3. O on the 10-membered ring	5.30	-1.36	5.30	-0.65
4. O of H-O-Si	4.00	-1.71	4.10	-0.62
5. H of H-Si	3.90	-0.74	3.60	-0.61
6. H of H-O	4.10	-0.47	3.30	-1.31
H of CH_4 Points toward/Away from the Center of the Ring				
7. E2	5.90	-1.94	6.30	-1.24
8. E3	4.90	-1.23	4.60	-1.68
9. E4	5.40	-2.54	5.40	-2.12
H of CH_4 Points toward/Away from the Center of the 10-Membered Ring				
10. E0	0.00	-4.26	0.8	-5.75

mol with the D_{opt} distance (from the C atom of the methane to the O atom of the silanol group) of 4.00 Å. Due to a very weak interaction between the methane molecule and the hydrophilic silanol covered surface of the silicalite-1, the potential energy curve shows a very broad minimum. Examples are the MP2 and the ONIOM binding energies for the E3 ring shown in Figure 4b. Therefore, a clear conclusion, in terms of the binding energy and the optimal distance, cannot be made because the energy of binding in different trajectories and orientations lies within the range of the thermal fluctuation at room temperature. Note that kT at room temperature is about 2.5 kJ/mol where T denotes the temperature in Kelvin and k is Boltzmann's constant.

For the trajectories pointing to the centers of small size channels, E2–E4 rings, the most stable binding site is situated at the center of the E4 ring (path 9 in Table 1) in the configuration H-in. The corresponding binding energy and distance are -2.54 kJ/mol and 5.40 Å, respectively.

Considering the path E0 in which the methane molecule moves to the center of the straight channel, more details were additionally investigated and plotted in Figure 5. In the configuration H-in (solid line in Figure 5), the first minimum was detected at the D_{opt} (from C atom of methane to center of the E0 ring) of 2.90 Å. At shorter distance, repulsion between

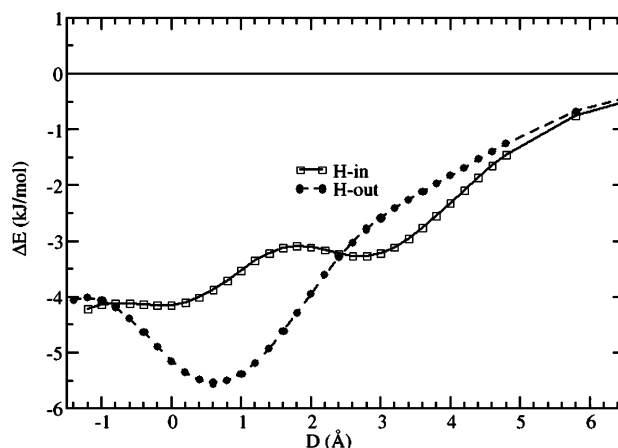


Figure 5. Binding energies ΔE_{bind} when the methane molecule is in the configurations H-in and H-out (Figure 3b) and moves perpendicular to the center of the E0 ring (Figure 3a), where D_{opt} denotes the distance from the C atom of methane to the center of the E0 ring.

the H atoms of methane and the atoms of the 10-oxygen membered ring leads to a slight increase of the binding energy. After a broad maximum at $D_{\text{opt}} = 1.80 \text{ \AA}$ the binding energy, again, decreases and remains constant at -4.14 kJ/mol between $D_{\text{opt}} = 0.0$ and -1.50 \AA (minus value of the D_{opt} denotes the position where the methane molecule is under the surface). Note that at $D_{\text{opt}} = 0.0 \text{ \AA}$ in the H-in configuration, the C atom of methane is located at the center of the straight channel.

For the configuration where one H-atom of methane points away from the surface, H-out, the binding energy decreases rapidly when D_{opt} decreases. The minimum was found when the three hydrogen atoms of methane are in the E0 plane; i.e., the distance to the C atom of methane, D_{opt} , is 0.60 \AA and the corresponding energy is -5.75 kJ/mol . This is the optimal binding between the methane and the silanol covered (001) surface based on the ONIOM (MP2/6-31G(d):HF/6-31G(d)) calculation with the BSSE correction. At $D_{\text{opt}} < 0.60 \text{ \AA}$, the energy, again, increases. The H-out configuration gives a binding energy identical to that of the H-in one, -4.15 kJ/mol , when the C atom locates below the surface $D_{\text{opt}} = -1.00 \text{ \AA}$ and one of the H-atom lies in the silicalite-1 surface. Note, however, that in this study we examine only the influence of the external sheet of atoms of the lattice on the approach of the methane molecule. Therefore, the energies obtained from this work cannot be compared to the experimental adsorption energy because we examine the influence of the surface only. All atoms of the silicalite-1 lattice would contribute to the complete adsorption process.

The calculated energies are higher than those from refs 33 and 34 where only a small fragment was used. This can be due to the effect of the hydrogen atoms which were added to saturate the broken terminal bonds.

4. Conclusion

Quantum chemical calculations were carried out to seek for the optimal binding site and orientation as well as the binding energy of a methane molecule on the silanol covered (010) surface of silicalite-1. The ONIOM (MP2/6-31G(d):HF/6-31G(d)) method with the correction of the basis superposition errors was found to be a compromise between the accuracy and computer time required for the investigated system. The ONIOM binding energies and distances are almost the same as those yielded from the MP2 calculations using the same fragment size as that of the real part of the ONIOM method. The optimal binding site is located at the straight channel and the binding energy is significantly lower than that of the other regions; therefore, the methane molecule was suggested to move freely above the surface and enter into the straight channel in the configuration pointing one of the H-atoms to the center of the straight channel.

Acknowledgment. We acknowledge the use of computing facilities provided by the Computing Center of the Leipzig University. This work was financially supported by the National Research Council of Thailand (NRCT), the Deutsche Forschungsgemeinschaft (DFG FR1486/1) and the Thailand Research Fund (TRF).

References and Notes

(1) Takaba, H.; Koshita, R.; Mizukami, K.; Oumi, Y.; Ito, N.; Kubo, M.; Fahmi, A.; Miyamoto, A. *J. Membr. Sci.* **1997**, *134*, 127.

- (2) Smirnov, K. S. *J. Phys. Chem. B* **2001**, *105*, 7405.
 (3) Takaba, H.; Koyama, A.; Nakao, S. *J. Phys. Chem. B* **2000**, *104*, 6353.
 (4) Armaroli, T.; Bevilacqua, M.; Trombetta, M.; Milella, F.; Alejandre, A. G.; Ramirez, J.; Notari, B.; Willey, R. J.; Busca, G. *Appl. Catal. A* **2001**, *216*, 59.
 (5) Simon, J. M.; Decrette, A.; Bellat, J. B.; Salazar, J. M. *Mol. Simul.* **2004**, *30*, 621.
 (6) Komiyama, M.; Kobayashi, M. *J. Phys. Chem. B* **1999**, *103*, 10651.
 (7) Chandross, M.; Webb, E. B., III; Grest, G. S.; Martin, M. G.; Thompson, A. P.; Roth, M. W. *J. Phys. Chem. B* **2001**, *105*, 5700.
 (8) Pieterse, J. A. Z.; Veeffkind-Reyes, S.; Seshan, K.; Lercher, J. A. *J. Phys. Chem. B* **2000**, *104*, 5715.
 (9) Tanaka, H.; Zheng, S.; Jentys, A.; Lercher, J. A. *Stud. Surf. Sci. Catal.* **2002**, *142*, 1619.
 (10) Turro, N. J. *Acc. Chem. Res.* **2000**, *33*, 637.
 (11) Turro, N. J.; Lei, X.; Li, W.; Liu, Z.; Ottaviani, M. F. *J. Am. Chem. Soc.* **2000**, *122*, 12571.
 (12) Park, S. H.; Rhee, H. K. *Catal. Today* **2000**, *63*, 267.
 (13) Klemm, E.; Scheidat, H.; Emig, G. *Chem. Eng. Sci.* **1997**, *52*, 2757.
 (14) Aguilar, J.; Corma, A.; Melo, F. V.; Sastre, E. *Catal. Today* **2000**, *55*, 255.
 (15) Denoyer, J. F.; Baron, G. V.; Vanbutsele, G.; Jacobs, P. A.; Martens, J. H. *Chem. Eng. Sci.* **1999**, *54*, 3553.
 (16) Zecchina, A.; Bordiga, S.; Spoto, G.; Marchese, L. *J. Phys. Chem.* **1992**, *96*, 4991.
 (17) Trombetta, M.; Busca, G.; Lenarda, M.; Storaro, L.; Pavan, M. *Appl. Catal. A* **1999**, *182*, 225.
 (18) Armaroli, T.; Bevilacqua, M.; Trombetta, M.; Milella, F.; Alejandre, A. G.; Ramirez, J.; Notari, B.; Willey, R. J.; Busca, G. *Appl. Catal. A* **2001**, *216*, 59.
 (19) Trombetta, M.; Armaroli, T.; Alejandre, A. G.; Solis, J. R.; Busca, G. *Appl. Catal. A* **2000**, *192*, 125.
 (20) Armaroli, T.; Trombetta, M.; Alejandre, A. G.; Solis, J. R.; Busca, G. *Chem. Phys.* **2000**, *2*, 3341.
 (21) Kawai, T.; Tsutsumi, K. *Colloid Polym. Sci.* **1998**, *276*, 992.
 (22) Olson, D. H.; Haag, W. O.; Borghard, W. S. *Microporous Mesoporous Mater.* **2000**, *35*, 435.
 (23) Trombetta, M.; Busca, G. *J. Catal.* **1999**, *187*, 521.
 (24) Nyfeler, D.; Armbruster, T. *Am. Mineral.* **1998**, *83*, 119.
 (25) Eisenberg, D.; Kauzmann, W. *The Structure and Properties of Water*; Oxford University Press: Oxford, U.K., 1969.
 (26) Wu, J.; Li, S.; Li, G.; Li, C.; Xin, Q. *Appl. Surf. Sci.* **1994**, *81*, 37.
 (27) Smit, B. *J. Phys. Chem.* **1995**, *99*, 5597 and references therein.
 (28) Saengsawang, O.; Remsungnen, T.; Fritzsche, S.; Haberlandt, R.; Hannongbua, S. *J. Phys. Chem. B* **2005**, *109*, 5684.
 (29) Baerlocher, Ch.; Meier, W. M.; Olson, D. H. *Atlas of Zeolite Framework Types*, 5th revised ed.; Elsevier: Amsterdam, 2001.
 (30) Hobza, P.; Zahradnik, R. *Chem. Rev.* **1998**, *88*, 871.
 (31) Sauer, J.; Ugliengo, P.; Garrone, E.; Saunders, V. R. *Chem. Rev.* **1994**, *94*, 2095.
 (32) Bussai, C.; Fritzsche, S.; Haberlandt, R.; Hannongbua, S. *J. Phys. Chem. B* **2004**, *108*, 13347.
 (33) Bussai, C.; Fritzsche, S.; Haberlandt, R.; Hannongbua, S. *Langmuir* **2005**, *21*, 5847.
 (34) Frisch, M. J.; Trucks, G. W.; Schlegel, H. B.; Scuseria, G. E.; Robb, M. A.; Cheeseman, J. R.; Montgomery, J. A., Jr.; Vreven, T.; Kudin, K. N.; Burant, J. C.; Millam, J. M.; Iyengar, S. S.; Tomasi, J.; Barone, V.; Mennucci, B.; Cossi, M.; Scalmani, G.; Rega, N.; Petersson, G. A.; Nakatsuji, H.; Hada, M.; Ehara, M.; Toyota, K.; Fukuda, R.; Hasegawa, J.; Ishida, M.; Nakajima, T.; Honda, Y.; Kitao, O.; Nakai, H.; Klene, M.; Li, X.; Knox, J. E.; Hratchian, H. P.; Cross, J. B.; Bakken, V.; Adamo, C.; Jaramillo, J.; Gomperts, R.; Stratmann, R. E.; Yazyev, O.; Austin, A. J.; Cammi, R.; Pomelli, C.; Ochterski, J. W.; Ayala, P. Y.; Morokuma, K.; Voth, G. A.; Salvador, P.; Dannenberg, J. J.; Zakrzewski, V. G.; Dapprich, S.; Daniels, A. D.; Strain, M. C.; Farkas, O.; Malick, D. K.; Rabuck, A. D.; Raghavachari, K.; Foresman, J. B.; Ortiz, J. V.; Cui, Q.; Baboul, A. G.; Clifford, S.; Cioslowski, J.; Stefanov, B. B.; Liu, G.; Liashenko, A.; Piskorz, P.; Komaromi, I.; Martin, R. L.; Fox, D. J.; Keith, T.; Al-Laham, M. A.; Peng, C. Y.; Nanayakkara, A.; Challacombe, M.; Gill, P. M. W.; Johnson, B.; Chen, W.; Wong, M. W.; Gonzalez, C.; Pople, J. A. *Gaussian 03*, revision C.02; Gaussian, Inc.: Wallingford, CT, 2004.
 (35) Monfort, X. S.; Sodupe, M.; Branchadell, V.; Sauer, J.; Orlando, R.; Ugliengo, P. *J. Phys. Chem. B* **2005**, *109*, 3545.